EXPERIMENTAL DESIGN APPROACH FOR STUDYING OVERHANGING FEATURES IN SELECTIVE LASER MELTING

A.E. Patterson[1], S.L. Messimer[1], P.A. Farrington[1], C.L. Carmen[2] and J.T. Kendrick[2]

[1]Department of Industrial & Systems Engineering and Engineering Management, University of Alabama in Huntsville, Huntsville, Alabama, 35899, USA.

[2]Department of Mechanical and Aerospace Engineering, University of Alabama in Huntsville, Huntsville, Alabama, 35899, USA.

Corresponding Author's Email: [1]albert.patterson@uah.edu

Article History: Received 3 August 2018; Revised 13 March 2019; Accepted 12 July 2019

ABSTRACT: As additive manufacturing (AM) processes become more refined and widely used, it is essential for engineers and designers to understand the processes in order to effectively use them within manufacturing systems; however, most of the existing methods for analyzing AM processes are too complex and specialized for use in practice. This study proposes a simple technique to derive information about the behavior of unsupported overhanging features in parts made using selective laser melting (SLM) using a first-principles finite element model and factorial experiment. This method can be used to assist with design decisions without production of prototypes, resulting in improved design and reduced cost. The case study presented examined five factors (laser power, laser spot size, scan speed, feature thickness, and the use of support material) in a 25 full-factorial arrangement with two stress and two deformation responses. An analysis of variance (ANOVA) was completed on the results, showing the significance of both the factors and the interactions between them. Two materials were studied (Ti-6Al-4V and 316L stainless steel). The results were compared to some similar stress and deformation results from experimental literature and were found to match well with the greatly simplified approach.

KEYWORDS: *SLM; Additive Manufacturing; Design of Experiments; Design for Manufacturability*

1.0 INTRODUCTION

A major challenge in implementing additive manufacturing (AM) methods lies with their use in engineering design [1]; the processes are often not well understood by either product designers or production

engineers, which limits their usefulness and applicability in practice. Many of these processes exist but engineers and designers are often reluctant to adopt them for fear of unknown complications or problems. Additive technologies have much to offer the production world beyond prototyping, with new possibilities in mass customization, design freedom, simplified supply chains, and elimination of specialized tooling [2]. A first step in this direction would be to equip engineering designers and production engineers with an appropriate tool to examine and judge the value of a manufacturing process within the scope of their work, a tool that can be applied easily and consistently across working groups and that has a universal meaning to stakeholders. One of the most useful and promising of the AM processes is the selective laser melting (SLM) process, a variation of the powder bed fusion family of AM processes, typically used to create full-density metal parts. There are many advantages to employing SLM, including fine detail resolution, good surface finish, customizability of the mechanical properties, and ability to handle materials that traditionally have low manufacturability such as nickel and titanium alloys [2-4]. SLM and other laser-powder-bed AM processes are a new type of application for laser-based manufacturing techniques, joining a number of well-established processes such as laser forming and laser welding [5-10]. Figure 1 shows the basic mechanics of the SLM process [11]; a digital model of the part to be made is input to the SLM machine, along with the raw material in the form of metal powder. The laser selectively scans the surface of the powder for each layer, fully melting the powder and producing solid geometry. After each layer is completed, a wiper and moving build plate deposits another layer of raw powder, which is then melted by the laser. This process continues until the part is completed.

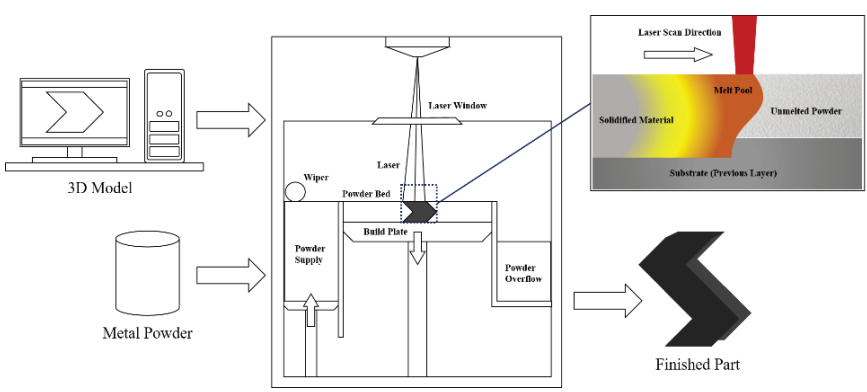

Figure 1: SLM process schematic [11]

However, the SLM process has a serious inherent problem: the process is extremely sensitive to the process control and input parameters; if the process is not very carefully controlled, the heat cycling of the fusing laser can introduce severe residual stresses into the material. These residual stresses can initiate part deformation, cracking, and delamination; these stresses can cause significant reduction of fatigue life or, in extreme cases, part self-destruction during or immediately after printing [12-13]. The most common way to deal with this problem, in practice, is to attach every feature to the build plate using solid and bulky support structures and perform stress relieving operations on the entire part before cutting it from the plate using an electric discharge machine or bandsaw [14]. This is a practical solution for simple parts, but the problem becomes far more complex when dealing with the stresses in overhanging features. A number of "fixes" have been devised to deal with these residual stresses without special post-processing operations or cumbersome, wasteful support structures; some of them attempt to directly control the process parameters while some are efforts to work around the process constraints; a comprehensive discussion of these methods can be found in [3, 11] and will not be reproduced here. While some of these solutions have been quite successful in particular cases, what is sorely needed is a general design-for-manufacturability (DFM) theory for SLM [15]. When designing parts that will be manufactured using any AM process (and especially so in very sensitive processes such as SLM), it is important to incorporate DFM principles whenever possible. DFM provides tools both for mitigating potential manufacturing problems from the inherent weaknesses of a process and for providing insight into extra design benefits that may be available when using a particular process [11, 15-17].

The present work offers four fundamental scholarly contributions: (1) a simple method for gathering design-valuable data on SLM overhang behavior which may be used in a design-for-manufacturability analysis, (2) demonstration of the collection and use of factor interaction data to understand factor impact in SLM, (3) demonstration of a process for selecting important/impactful process parameters in SLM, and (4) provision of some new conclusions about SLM overhang behavior from the developed model, particularly the strong negative impact on the stress responses when using support material and dependence of the overhang behavior on variations in material properties.

2.0 METHODOLOGY

2.1 Motivation and Approach

Part of the design of any experiment is the specification of a technique, usually in the form of an analysis of raw data taken during experimental runs. However, SLM is extremely difficult to experiment with in-situ, due to the fact that the chamber must remain oxygen-free and strictly undisturbed to work correctly [4]. Even with the use of thermal cameras, it is next to impossible to capture reliable data that is not subject to interpretation on the instantaneous stresses and deformations as they form in the part during printing. It is a simple matter to study the damage and deformation after the part is complete, but that does not give the instantaneous in-process perspective needed to understand SLM from the DFM perspective. Improvements are being made in this area [18] but a practical real-time solution is not widely available. Therefore, in order to capture a "snapshot" of the process in action in the most practical way without manufacturing thousands of dollars' worth of test parts, a thermo-mechanical Finite Element Analysis (FEA) model was built to simulate the SLM process in action at a particular point in time during the printing process. The energy input for the model is the laser power and the outputs range from thermal to stress and deformation results. FEA is a common method for studying AM processes in-run [12, 19-20].

2.2 Heat Transfer Model Development

The FEA model was generated using the SolidEdge® ST6 FEMAP® FEA tool. The required inputs for an FEA model are the loads, the initial conditions, and the boundary conditions. The loading for the present experiment was the laser input. The proper initial conditions were calculated using a simple thermal model based on the first principles of heat transfer, as seen in Figure 2. Assuming that the model is operating at approximately steady-state and that q_1 represents the heat input from the laser,

$$q_{in} - q_{out} = q_l - q_b - q_p - q_{air_{conv}} - q_{air_{rad}} = \frac{d}{dt} E_{total} = 0 \quad (1)$$

$$q_b = \frac{k_b A_{1-2}}{L_b}(T_1 - T_2) \quad (2)$$

$$q_p = \frac{k_p A_{1-2}}{L_p}(T_1 - T_2) \quad (3)$$

$$q_{air_{conv}} = \bar{h}_a A_{1-2}(T_1 - T_2) \quad (4)$$

$$q_{air_{rad}} = \varepsilon \sigma A_{1-2}(T_1^4 - T_2^4) \quad (5)$$

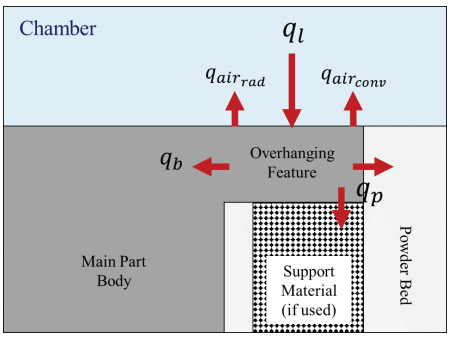

Figure 2: SLM heat transfer model

Where Equation (1) describes the basic energy balance of the system and Equations (2) and (3) describe the heat transfer between the overhanging feature and the part body and powder bed, respectively. Equations (4) and (5) describe the surface heat losses from convection and radiation from the surface of the part. k_b and k_p represent the thermal conductivity of the part body and powder bed, respectively, while $A_{1\text{-}2}$ is the heat transfer area from the overhanging feature to its surroundings. The length of the distance needed for heat to flow is represented by L_p and L_b, while the temperature gradients are specified by T_1-T_2. The convection and radiation parameters are represented by $\bar{h}_a$ (convection coefficient), ε (emissivity), and σ (Stefan-Boltzmass constant).

Boundary conditions were applied to the model to simulate the effects of the powder support or a support structure. Powder-only support was modeled as a pressure equal to the force of gravity, where the overhang was free to move up, but not down into the powder bed. The support material was simulated using full fixed constraints on the bottom surface of the overhang. It was assumed that the support

material did not provide enough contact area nor mass density to be significantly more conductive than the powder bed and provided only structural effects. Note that SLM requires an argon-filled chamber but was approximated by properties of air in this model.

2.3 Model Validation

Once the FEA model was set up, an in-depth verification and validation study was completed. A series of test scenarios were created, borrowing geometry, process settings, and results from published studies [12, 19, 21-23], from which the geometries, boundary conditions, inputs, and final outcomes were known. In most cases the results from the FEA model were similar to the studies but some adjustments to the values of the boundary conditions (such as initial temperatures) were prompted by a few of the runs. Once any needed adjustments were made to the boundary conditions and modeling assumptions, the results from the model and the test studies were very similar, so the FEA model was considered to be valid.

2.4 Experimental Design: Factors

Five factors or "main effects" were chosen for study after a review of the SLM literature [3, 11] to understand the experimental designs used in previous studies. The stated goal of the experiment is to provide a simple and easy-to-use model for design engineers and production managers and this outlook was essential in choosing which factors to examine. Many others could have been chosen, including layer thickness, but the five that appear to best represent the parameters set or evaluated by designers and managers were examined. The choice will be made by both engineers and management; the approach outlined in this paper facilitates this well, as it allows analysis of any important variables relative to each other and is not dependent on specific input variables. The variables and their levels for this study were (summary in Table 1):

i. Laser power: Modeled as a constant heat flux input into the FEA model
ii. Laser spot diameter: Modeled as an element on the surface of the material
iii. Laser scan speed: Heat flux is the load on the model, so the input must be known
iv. Thickness of the overhanging feature: The material thickness strongly affects the thermal gradient and the mechanical behavior of the material during processing

v. Support Structure: Support materials can often cause problems during design and processing and require extra resources to remove.

Table 1: Factors and levels

Factor		Low	High
A	Laser Power (Watts)	80	110
B	Laser Spot Diameter (μm)	26	50
C	Laser Scan Speed (mm/s)	200	300
D	Feature Thickness (mm)	2.5	5
E	Support Structure	No	Yes

2.5 Experimental Design: Materials

It was decided to set up the experiment for two runs, each modeling the use of a different material. Run 1 was set up to use TI-6V-4Al and Run 2 was set up to use 316L stainless steel, two commonly used materials in SLM. It was decided to keep the materials separate and not include them as an extra factor in the experimental design; this allowed the final results of the experiment to be more easily validated by being compared with the theory and with single-material published studies on SLM. In SLM, the material properties cannot be assumed to follow the standard material datasheets, due to the heat cycling and strain hardening experienced by the material; for the present study, a survey of SLM-related characterization studies [12, 23-32] was conducted to collect experimentally-verified properties. The results are shown in Table 2; the shown properties are averages and were used as inputs into the FEA model. It should be noted that appropriate settings were pre-selected within the FEA software to account for heat of fusion and the gradients in material properties as the material is heated.

Table 2: Material properties used in model

Property	Ti-6Al-4V	316L SS	Source
Density (kg/m^3)	4421.3	7923	Average value from [12, 22-31]
Yield strength (MPa)	1083.3	588.4	
Elastic modulus (GPa)	113.8	193.0	Datasheet values from [25-27]
Thermal expansion (m/m-k)*10^6	9.2	17.0	
Specific heat (J/kg-K)	526.3	500.0	
Thermal conductivity (solid) (W/m-K)	16.8	18.8	
Thermal conductivity (powder) (W/m-K)	2.50	1.67	
Surface emissivity	0.325	0.250	
Melting point (°C)	1604.0	1371.0	

2.6 Experimental Design: Responses

Responses were chosen after group discussions about important part design parameters:

i. The in-process Von Mises stress ("MP Stress") near the melt spot but still in a non-molten area of the part.
ii. The Von Mises stress 5mm away from the pool ("CF Stress") into the recently scanned area to read heat gradient effects on stress throughout the overhang.
iii. The Z-direction deformation of the material immediately surrounding the melt pool ("MP Deformation") in order to deduce if enough stress was produced to plastically deform the part.
iv. The Z-direction deformation at the furthest overhanging point on the feature ("EF Deformation") from the melt pool to understand the influence of support material.

2.7 Experimental Model

Figures 2 and 3 demonstrate the details and model of the geometry under study, including the factors and responses. The time-dependent nature of the responses is converted to non-time-dependent by using the aforementioned FEA model to measure all of the responses at the same point in time in the printing. While this does not give a "simulation" of the SLM process as a function of time, it does allow all of the input factors and their interactions to be studied relative to the instantaneous responses and to each other; this allows the impact of each factor and each interaction on the responses to be captured, accomplishing the goals of this study. The most important assumption for this type of model is that the heat transfer and the material physics behave approximately the same in each layer of the part, with the caveat that enough solid material exists beneath the layer in progress to effectively transfer the heat like a fin; this has been determined to be 0.5-0.9mm [12, 22] or approximately 10-15 layers.

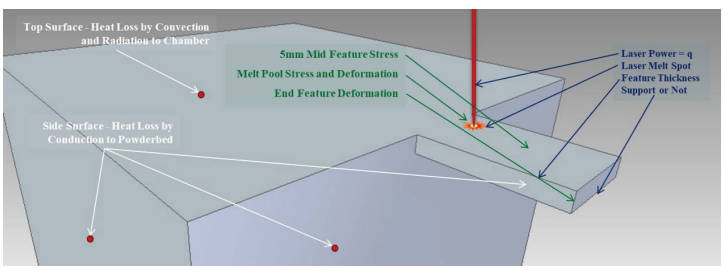

Figure 3: Experimental model

2.8 Level of Significance

For the present study, a model adequacy level of significance of α = 0.05 was chosen to be used to verify the ANOVA [33]. A much more subjective decision is the selection of the level of significance for the ANOVA, as this choice is based on the circumstances and goals of the experiment. The purpose of the present study was to develop an engineering design tool, so it is imperative that the experiment provides the widest possible view of the process to designers. Therefore, it is vital to reduce the possibility of committing Type II errors (false rejection of a significant factor); the probability of avoiding Type II errors is known as the "power of the experiment". Increasing the power also increases the probability of making a Type I error (false acceptance of an insignificant factor), but this was judged acceptable for this experiment; any falsely accepted insignificant factors will remain insignificant and will not influence the outcome of the process, as the missing of a significant factor would be. Therefore, to reduce the possibility of false rejections to the lowest feasible level, it was decided to use α = 0.25 for the ANOVA tests [3, 34-35].

2.9 Experimental Runs

Following the basic set of assumptions and approximations for such an SLM model, such as those described in references [3, 12, 19, 22, 35], numerical experiments were run. Loading the CAD model into the FEA software and applying the initial and boundary conditions were the first steps for each run. The experiment was run 32 times each for the Ti-6Al-4V and 316L stainless steel materials, with the four responses for each run, for a total output of 256 data points; the basic experimental procedure is shown as a flowchart in Figure 4a. The planning, setup, execution, and data collection required approximately 80 hours to complete and were conducted over a period of three weeks. Views of the experiment during the execution phase in one of the runs are shown in Figures 4b (stress) and 4c (deformation). The full collected dataset from the experiments can be found in Figure 5.

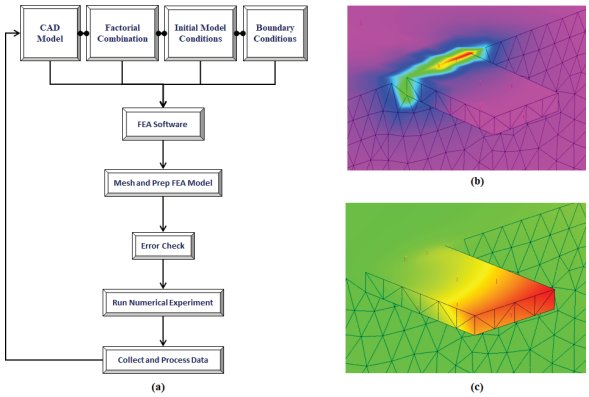

Figure 4: (a) Experimental data collection procedure and in-process examples of (b) stress and (c) deformation responses

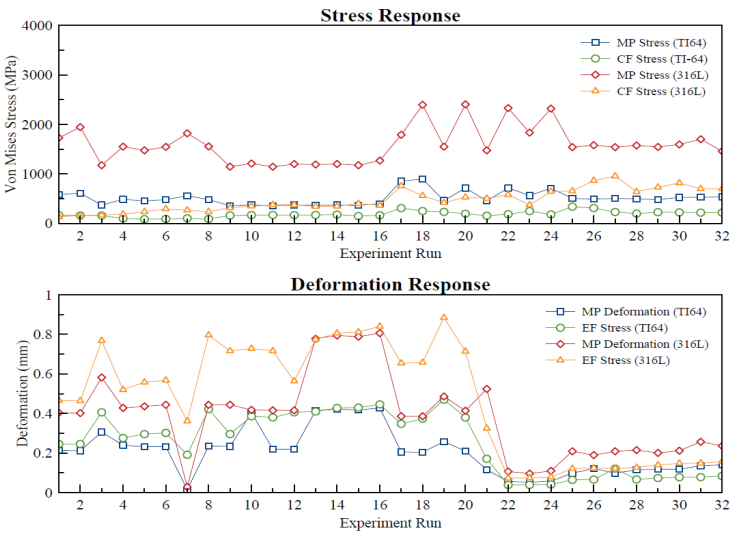

Figure 5: Collected experimental data for the stress and deformation responses (response definitions given in Section 2.6)

3.0 RESULTS AND DISCUSSION

Once the experiment was complete, the data (Figure 5) was checked for severe skewing and outliers, and other indications that errors were made in the conduct and collection of the experiment. None were found, so the recorded data was divided into eight groups: one for each response for each material under study. Each of the eight subsets was then checked and subjected to a residual analysis using Minitab® to verify the model adequacy and perform a preliminary check for significant factors and interactions. The model adequacy was immediately established in seven of the eight cases, while a Box-Cox

transform was needed to show the adequacy of the model for the eighth case. A more detailed presentation of this technique and the procedure for model adequacy testing can be found in [3, 33]. Tables 3 and 4 show the results of all eight of the ANOVAs that were conducted during the present study; the list of potentially significant factors and interactions is shown in Table 3, while the observed set of significant factors and interactions are given in Table 4.

Table 3: Set of factors and potential significant interactions

Main Factors	Potential Interactions (up to 5th order)					
A	A*B	A*C	A*D	A*E	B*C	B*D
B	B*E	C*D	C*E	D*E	A*B*C	A*B*D
C	A*C*D	B*C*D	A*B*E	A*C*E	B*C*E	A*D*E
D	B*D*E	C*D*E	A*B*C*D	A*B*C*E	A*B*D*E	A*C*D*E
E	B*C*D*E	A*B*C*D*E				

Table 4: Observed set of significant factors/interaction for the SLM experiment

Material	Response	Significant Factors (α = 0.25)	Significant Interactions (α = 0.25)
Ti-6Al-4V	Melt Pool Stress	A, B, C, D, E	B*C, B*D, C*D, B*C*D
	Central Feature Stress	B, C, D, E	B*C, B*E, C*E, B*C*E
	Melt Pool Deformation	D, E	C*D, C*E, D*E, A*B*C, A*C*D, B*C*D
	End Feature Deformation	B, C, D, E	A*C, A*D, A*E, B*C, C*D, C*E, D*E, A*B*C, A*C*D, A*C*E, C*D*E, A*C*D*E
316L Stainless Steel	Melt Pool Stress	A, D, E	A*C, A*D, A*E, B*C, A*B*C, B*C*D, A*D*E
	Central Feature Stress	D, E	A*C, B*D, C*E, D*E, A*B*D, A*C*E, A*B*D*E
	Melt Pool Deformation	D, E	A*B, A*E, B*C, B*D, C*D, C*E, D*E, A*B*C, A*B*D, B*C*D, A*B*E, A*C*E, C*D*E, A*B*C*D
	End Feature Deformation	C, D, E	A*E, B*C, B*D, C*D, C*E, D*E, A*B*C, B*C*D, A*B*E, A*C*E, C*D*E, A*B*C*D

With the exception of the feature thickness factor, it was known at the beginning of the experiment that the chosen factors were likely to have significant influence on the generic SLM process from reviewed studies [12, 21, 35-36]. The feature thickness was added because it was an obvious design consideration and had not been explored in any of the many studies reviewed by the present authors. The raw output values of the stress and deformation were reasonable and similar to those found in previous studies; four of the responses had equivalent conditions and responses in other studies including material choice, which aided in evaluation of the findings. These are shown in Figure 6. In all shown cases, the red bars indicate the range of values found in indicated previous studies [12, 35] and the blue markers show the

data taken in the present work. The use of supports in the present experiment has a clear influence, which is most obvious in Runs 17-32 in the comparisons with Kruth et al. [35]. Note that the overhang geometry contains severe stress concentrations, so the overhang stress readings will be significantly higher than they would be in a more generic geometry.

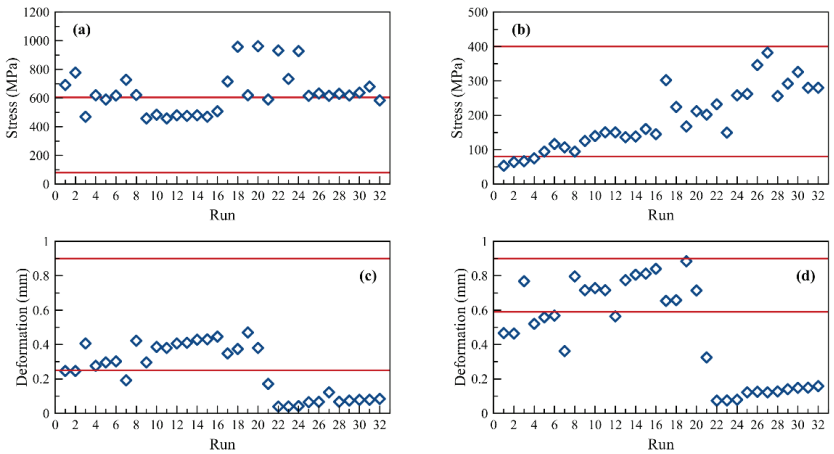

Figure 6: Results compared with experimental data, (a) melt pool stress compared with [12], (b) central feature stress compared with [12], (c) end feature deformation (Ti-6Al-4V) compared with [35] and (d) end feature deformation (316L) compared with [35]

To compare the data with the studies in question, the raw values of the data were transformed by dividing them by the stress concentration factor, which was taken to be 2.5, an average textbook value for this kind of geometry. This way, the influence of the manufacturing process can be studied separately from the geometric influences and compared to experimental data. This transform explains the difference between the stress data shown in Figure 5 with that in Figure 6. It should be re-stated that the goal of this experiment is not to collect technical or material process data but to provide a new perspective for designers and production engineers to judge and evaluate the value of SLM within their production system. The purpose of analyzing technical data here is to provide further validation of the model and its relationship information. In practice, the model would be used to collect decision data such as experimental factors, interactions, and their p-values for comparison.

There were five major findings from the present experiment. First was the fact that the feature thickness has a major influence on all of the responses, which had not been tested previously in other studies.

The dominantly significant factor for an overhanging feature was its thickness. The second and most surprising of these findings was that the laser power had such a small influence upon the responses; it was found to only have any type of influence on the stress responses directly around the melt pool. The third important finding in this study was the influence of the factor interactions. One of the major advantages of using full factorial experiments to conduct this type of study is the ability to study the interactions between the factors, as well as the factors themselves. It is very clear from the findings of the present study that there are many significant interactions for each response; historically, this is not often considered in SLM studies, depriving a typical study of an extra dimension of view concerning SLM behavior. Using the ANOVA to determine significance weighed each interaction equally with each factor, demonstrating clearly that some of the interactions between factors can have much influence on the experiment and an interaction can be significant even if its constituents are not significant. The determination of all the important design inputs is important to the creation of a generalized DFM methodology for SLM and it is obvious that the interactions between factors, even insignificant factors, are worthy of much further study; in the present study, there were an average of 1.73 significant interactions per significant factor for Ti-6Al-4V and 3.8 per significant factor for 316L stainless steel.

The fourth major finding from this study was the large influence that specific material properties, particularly the yield and tensile strength, have on the stress and deformation responses from the overhanging feature. Figure 5 demonstrated this clearly: the stress response plot for the stainless steel shows a much larger difference between the melt pool stress and the central feature stress than what is seen for the titanium (Table 2), this difference is inversely proportional to the differences in yield and tensile strength for the two materials. A similar effect can be observed in the unsupported runs of the deformation responses (Figure 5). This is a very important consideration for designing for SLM, as the final part properties can vary significantly between processes and machines; the best example is the material properties collected in Table 2; in this case, the titanium alloy is actually more ductile on average than the stainless steel, while stainless steel is one of the most ductile engineering materials when bulk-formed. The effect of the material choice on the likelihood of having significant factor interactions is also shown in the results presented in Table 3: for the titanium alloy, the probability of a main effect being significant is 0.75, while the probability of an interaction being significant is 0.25; for the stainless steel, the probabilities are 0.50 and 0.37.

The fifth and final finding was that a complex relationship exists between the use of support material and in-process stress and deformation. The right half (Runs 17-32) of the response plots (Figure 5) were runs during which solid support material was added to the model to attach the overhang to the build plate. It is obvious, from inspecting the raw data, that the support material had a huge influence on the responses; the most obvious result of adding support is that decreasing the deformation causes the stresses to increase and become less uniform in nature. According to Lachin [34], this stress cycling caused by repeated scans by the laser is precisely what causes the major residual stresses to be introduced in the first place. Further studies are needed in this area, but the results of the present study suggest that adding support materials may actually increase the probability of introducing damaging residual stresses into an overhanging or protruding part feature. This must be carefully considered by designers using SLM.

4.0 CONCLUSION

It is clear that the information gathered and presented by this model is valuable to design engineers and production managers using or considering the use of SLM; it can be used for many other problems besides the design and production of overhanging features. This information would be very difficult and costly to extract out of a large series of specialized studies and to translate into a form that is useful in a business-industrial setting. Users of this technique will be able to quickly and easily examine or predict the outcomes of the SLM process in a way that is easily communicable with non-specialists. Further development of the method is needed, including comprehensive (and very expensive) experimental verification.

ACKNOWLEDGEMENTS

The authors thank Robert Renz for advice on the formulation of the thermo-mechanical model and James Swain for guidance on the experimental design and level of significance selection. An earlier version of a portion of this work was presented in the thesis “Design of experiment to analyze effect of input parameters on thermal stress and deformation in overhanging part features created with the SLM additive manufacturing process” [3] defended by Albert E. Patterson at the University of Alabama in Huntsville in 2014.

REFERENCES

[1] M.K. Thompson, G. Moroni, T. Vaneker, G. Fadel, R.I. Campbell, I. Gibson, A. Bernard, J. Schulz, P. Graf, B. Ahuja and F. Martina, "Design for additive manufacturing: Trends, opportunities, considerations, and constraints," *CIRP Annals*, vol. 65, no. 2, pp. 737-760, 2016.

[2] N. Guo and M. Leu, "Additive manufacturing: Technology, applications, and research needs," *Frontiers in Mechanical Engineering*, vol. 8, no. 3, pp. 215-243, 2013.

[3] A.E. Patterson, "Design of experiment to analyze effect of input parameters on thermal stress and deformation in overhanging part features created with the SLM additive manufacturing process," M.S. thesis, Department of Industrial & Systems Engineering and Engineering Management, University of Alabama in Huntsville, Huntsville, Alabama, USA, 2014.

[4] W. Meiners, K. Wissenbach and A. Gasser, "Selective laser sintering at melting," U.S. Patent No. 6,215,093. Washington, DC: U.S. Patent and Trademark Office, 2001.

[5] M. Safari and M. Farzin, "Experimental investigation of laser forming of a saddle shape with spiral irradiating scheme," *Optics & Laser Technology*, vol. 66, pp. 146-150, 2015.

[6] M. Safari, H. Mostaan and M. Farzin, "Laser bending of tailor machined blanks: Effect of start point of scan path and irradiation direction relation to step of the blank," *Alexandria Engineering Journal*, vol. 55, no. 2, pp. 1587-1594, 2016.

[7] H. Mostaan, M. Shamanian, S. Hasani, M. Safari and J.A. Szpunar, "Nd:YAG laser micro-welding of ultra-thin FeCo-V magnetic alloy: Optimization of weld strength," *Transactions of Nonferrous Metals Society of China*, vol. 27, no. 8, pp. 1735-1746, 2017.

[8] M. Safari and H. Mostaan, "Experimental and numerical investigation of laser forming of cylindrical surfaces with arbitrary radius of curvature," *Alexandria Engineering Journal*, vol. 55, no. 3, pp. 1941-1949, 2016.

[9] M. Safari, M. Farzin and H. Mostaan, "A novel method for laser forming of two-step bending of a dome shaped part," *Iranian Journal of Materials Forming*, vol. 4, no. 2, pp. 1-14, 2017.

[10] M. Safari and J. Joudaki, "Prediction of bending angle for laser forming of tailor machined blanks by neural network," *Iranian Journal of Materials Forming*, vol. 5, no. 1, pp. 47-57, 2018.

[11] A.E. Patterson, S.L. Messimer and P.A. Farrington, "Overhang Features and the SLM/DMLS Residual Stresses Problem: Review and Future Research Need," *Technologies*, vol. 5, no. 2, pp. 15, 2017.

[12] A. Hussein, L. Hao, C. Yan and R. Everson, "Finite element simulation of the temperature and stress fields in single layers built without-support in selective laser melting," *Materials & Design*, vol. 52, pp. 638-647, 2013.

[13] P. Mercelis and J.P. Kruth, "Residual stresses in selective laser sintering and selective laser melting," *Rapid Prototyping Journal*, vol. 12, no. 5, pp. 254-265, 2006.

[14] R. Sundar, P. Hedaoo, K. Ranganathan, K. Bindra and S. Oak, "Application of Meshes to Extract the Fabricated Objects in Selective Laser Melting," *Materials and Manufacturing Processes*, vol. 29, no. 4, pp. 429-433, 2014.

[15] G. Adam and D. Zimmer, "Design for Additive Manufacturing – Element transitions and aggregated structures," *CIRP Journal of Manufacturing Science and Technology*, vol. 7, no. 1, pp. 20-28, 2014.

[16] D. Rosen, "Computer-Aided Design of Additive Manufacturing of Cellular Structures," *Computer-Aided Design & Applications*, vol. 4, no. 5, pp. 585-594, 2007.

[17] K. Salonitis, "Design for additive manufacturing based on the axiomatic design method," *The International Journal of Advanced Manufacturing Technology*, vol. 87, no. 5, pp. 989-996, 2016.

[18] T. Craeghs, S. Clijsters, E. Yasa, F. Bechmann, S. Berumen and J-P. Kruth, "Determination of geometrical factors in Layerwise Laser Melting using optical process monitoring," *Optics and Lasers in Engineering*, vol. 49, no. 12, pp. 1440-1446, 2011.

[19] M. Matsumoto, M. Shiomi, K. Osakada and F. Abe, "Finite element analysis of single layer forming on metallic powder bed in rapid prototyping by selective laser processing," *International Journal of Machine Tools & Manufacture*, vol. 42, no. 1, pp. 61-67, 2002.

[20] E. Mirkoohi, J. Ning, P. Bocchini, O. Fergani, K-N. Chiang and S.Y. Liang, "Thermal modeling of temperature distribution in metal additive manufacturing considering effects of build layers, latent heat, and temperature-sensitivity of material properties," *Journal of Manufacturing and Materials Processing*, vol. 2, no. 3, pp. 63, 2018.

[21] D. Dai and D. Gu, "Thermal behavior and densification mechanism during selective laser melting of copper matrix composites: simulation and experiments," *Materials & Design*, vol 55, pp. 482-491, 2014.

[22] N. Contuzzi, S. Campanelli and A. Ludovico, "3D finite element analysis in the selective laser melting process," I*nternational Journal of Simulation and Modelin*g, vol. 10, no. 3, pp. 113-121, 2011.

[23] B. Zhang, L. Dembinski and C. Coddet, "The study of the laser parameters and environment variables effect on mechanical properties of high compact parts elaborated by selective laser melting 316L powder," *Materials Science & Engineering A*, vol. 584, pp. 21-31, 2013.

[24] P. Edwards and M. Ramulu, "Fatigue performance evaluation of selective laser melted Ti-6Al-4V," *Materials Science & Engineering A*, vol. 598, pp. 327-337, 2014.

[25] H. K. Rafi, T.L. Starr and B.E. Stucker, "A comparison of the tensile, fatigue, and fracture behavior of Ti-6Al-4V and 15-5 PH stainless steel parts made by selective laser melting," I*nternational Journal of Advanced Manufacturing Technology*, vol. 69, no. 5-8, pp. 1299-1309, 2013.

[26] Aerospace Specification Metals. (2018). Titanium TI-6AL-4V-AMS-4911 Datasheet [Online]. Available: http://www.aerospacemetals.com/titanium-ti-6al-4v-ams4911.html

[27] ATK Steel Corporation. (2018). 316/316L Stainless Steel Datasheet [Online]. Available: www.aksteel.com/pdf/markets_products/stainless/austenitic/316_316l_data_bulletin.pdf

[28] Engineering Toolbox. (2018). Young's Modulus-Tensile and Yield Strength for Common Materials. [Online]. Available: http://www.engineeringtoolbox.com/young-modulus-d_417.html

[29] C. Qui, N.J.E. Adkins and M.M. Attallah, "Microstructure and tensile properties of selective laser-melted and of HIPed laser-melted Ti-6Al-4V," *Materials Science & Engineering A*, vol. 578, pp. 230-239, 2013.

[30] A. Riemer, S. Leuders, M. Thone, H.A. Richard, T. Troster and T. Niendorf, "On the fatigue crack growth behavior in 316L stainless steel manufactured by selective laser melting," *Engineering Fracture Mechanics*, vol. 120, pp. 15-25, 2014.

[31] A.B. Spierings, N. Herres and G. Levy, "Influence of the particle size distribution on surface quality and mechanical properties in AM steel parts," *Rapid Prototyping Journal*, vol. 17, no. 3, pp. 195-202, 2011.

[32] I. Tolosa, F. Garciandia, F. Zubiri, F. Zapirain and A. Esnaola, "Study of mechanical properties of AISI 316 stainless Steel processed by "selective laser melting", following different manufacturing strategies," *International Journal of Advanced Manufacturing Technology*, vol. 51, no. 5-8, pp. 639-647, 2010.

[33] D. Montgomery, *Design and Analysis of Experiments*. Hoboken, NJ: John Wiley and Sons Publishers, 2001.

[34] J.M. Lachin, "Introduction to sample size determination and power analysis for clinical trials," *Controlled Clinical Trials*, vol. 2, no. 2, pp. 93-113, 1981.

[35] J.P. Kruth, J. Deckers, E. Yasa and R. Wauthle, "Assessing and comparing influencing factors of residual stresses in selective laser melting using a novel analysis method," *Proceedings of the Institution of Mechanical Engineers, Part B: Journal of Engineering Manufacture*, vol. 226, no. 6, pp. 980-991, 2012.

[36] J. Jhabvala, E. Boillat, C. André and R. Glardon, "An innovative method to build support structures with a pulsed laser in the selective laser melting process," International Journal of Advanced Manufacturing Technology, vol. 59, pp. 137–142, 2012.